HHS Public Access

Author manuscript

Nano Lett. Author manuscript; available in PMC 2018 June 18.

Published in final edited form as:

Nano Lett. 2010 May 12; 10(5): 1677–1681. doi:10.1021/nl100004m.

New insights on transmembranal mechanism and subcellular localization of noncovalently modified single-walled carbon nanotubes

Feifan Zhou[1], **Da Xing**[1,*], **Baoyan Wu**[1], **Shengnan Wu**[1], **Zhongmin Ou**[1], and **Wei R. Chen**[1,2,*]

[1]MOE Key Laboratory of Laser Life Science & Institute of Laser Life Science, College of Biophotonics, South China Normal University, Guangzhou 510631, China

[2]Biomedical Engineering Program, Department of Engineering and Physics, College of Mathematics and Science, University of Central Oklahoma, Edmond, OK 73034, USA

Abstract

Translocation and localization of single-walled carbon nanotubes (SWNTs) in normal and cancerous cells have significant biomedical implications. In this study, SWNTs functionalized with different biomolecules in cells were observed with confocal laser scanning microscopy. Functionalized with PL-PEG, SWNTs were found to localize exclusively in mitochondria of both tumor and normal cells due to mitochondrial transmembrane potential, but they were found mainly in lysosomes of macrophages due to phagocytosis. However, when conjugated with different molecules, the subcellular localization of the surface-modified SWNT-PL-PEG depended on how SWNTs enter the cells: inside mitochondria if crossing cell membrane or inside lysosomes if being endocytosized. We also show that mitochondrial SWNT-PL-PEG, when irradiated with a near-infrared light, can induce cell apoptosis due to mitochondrial damages. These findings provide a better mechanistic understanding of cellular localization of SWNTs, which could lead to advanced biomedical applications such as the design of molecular transporters and development of SWNT-assisted cancer therapies.

Keywords

Single-walled carbon nanotubes (SWNTs); subcellular localization; transmembranal mechanism; mitochondria; lysosomes

Single-walled carbon nanotubes (SWNTs) have been considered for various biomedical applications[1–5]. As a unique quasi one-dimensional material, SWNTs have been explored as

*Correspondence: Da Xing, Tel: +86-20-85210089; Fax: +86-20-85216052, xingda@scnu.edu.cn; Wei R. Chen, Tel: +1-405-974-5147; Fax: +1-405-974-3824, wchen@uco.edu.

Author Contributions

Feifan Zhou, Da Xing and Wei R. Chen conceived and designed the experiments.

Feifan Zhou and Shengnan Wu performed the cellular experiments.

Baoyan Wu and Zhongmin Ou constructed the SWNTs system.

Daniel E. Resasco and Yongqiang Tan provided the CoMoCAT SWNTs and performed the AFM/TEM experiments.

Feifan Zhou, Da Xing, and Wei R. Chen analyzed the data.

Feifan Zhou and Wei R. Chen prepared the manuscript.

novel delivery vehicles for drugs[8–10], peptides[6], proteins[7], plasmid DNA[11], and small interfering RNA[12], via endocytosis[7, 13]. The absorption spectrum of SWNTs in the near-infrared (NIR) region has been used for cell destruction[14–16]. Their NIR photoluminescence property has been used for in vitro cell imaging[17]. However, as the basis of biomedical applications of SWNTs, their translocation and localization in cells have not been fully understood.

Using transmission electron microscopy (TEM), Porter *et al* observed that HiPco SWNTs dispersed in tetrahydrofuran (THF) could cross the membranes of macrophages and localize in the lysosome, and they could even enter the nucleus[18]. Pantarotto *et al* reported that functionalized carbon nanotubes (CNTs) with fluorescein isothiocyanate (FITC), a fluorescent tag, dispersed in 1,3-dipolar cycloaddition of azomethine ylides could cross the membranes of living cells[6], although the specific subcellular localization of SWNTs was not clear.

Using confocal laser scanning microscopy, we observed SWNTs, dispersed in phospholipid-polyethylene glycol (PL-PEG) and conjugated with different molecules, in tumor, normal, and macrophage cells, to determine the subcellular localization and to study the transmembranal mechanism of SWNTs. We found that SWNT-PL-PEG-FITC were localized exclusively in the mitochondria of both tumor and normal cells due to mitochondrial transmembrane potential. The mitochondrial SWNT-PL-PEG, when irradiated with a near-infrared light, could induce cell apoptosis due to mitochondrial damages. We also demonstrated that SWNT-PL-PEG could be localized in different subcellular components by conjugations of different molecules. Our study should have a significant impact on designing molecular transporters and on developing SWNT-assisted cancer therapies.

To observe subcellular translocation of SWNT-PL-PEG-FITC, HeLa cells cultured in DMEM medium at 37°C were incubated with different combinations of FITC, PL-PEG and SWNTs. Subsequently, the cells were rinsed with PBS to remove unincorporated chemicals. Confocal images of the HeLa cells (Fig. S1, Supporting Information) show that SWNT-PL-PEG-FITC accumulates mainly in the cytoplasm, while free FITC and PL-PEG-FITC are absent inside the cells. The stability of localization of SWNT-PL-PEG-FITC in cells is shown by the confocal images of cells over a period of 96 hours (Fig. S2, Supporting Information).

To confirm the subcellular localization of SWNT-PL-PEG-FITC, HeLa cells transfected with DsRed-ER (to label Endoplasmic Reticulum), DsRed-Golgi (to label Golgi), CFP-lamp (to label lysosome), or stained with MitoTracker (to label mitochondria), were incubated with SWNT-PL-PEG-FITC for 30 minutes. Confocal images of the cells in Fig. 1A show that fluorescence emissions of SWNT-PL-PEG-FITC coincide with that of MitoTracker dye, indicating that SWNT-PL-PEG-FITC is only localized in mitochondria, not in any other subcellular component.

To determine the cell line dependence of subcellular localization of SWNT-PL-PEG-FITC, different cells (ASTC-a-1, MCF 7, COS 7, EVC304, and RAW264.7) were stained by

MitoTracker and incubated with SWNT-PL-PEG-FITC for 30 minutes, and observed under the microscope. Fig.1B shows that fluorescence emissions of SWNT-PL-PEG-FITC from either tumor cells or normal cells coincide with that of MitoTracker dye. However, in macrophages, lysosomes were the main source of fluorescence emissions (Fig. 1C). The observed lysosomal distribution of SWNT-PL-PEG-FITC in macrophages is consistent with the observation by Porter *et al*[18]. We attribute this phenomenon to the phagocytosis function of macrophages, since SWNT-PL-PEG-FITC were swallowed as foreign bodies and entered the lysosomes, as shown in Fig. 1C. We also observed some fluorescence emissions of SWNT-PL-PEG-FITC in the mitochondria (Fig. 1C upper), indicating that the SWNT-PL-PEG-FITC could also enter cells and localize in the mitochondria, although only in the phagocytosis cells.

To investigate the possible pathway for SWNTs translocation and localization, HeLa cells were either maintained at 4°C or incubated with NaN_3 at 37°C, followed by incubation with SWNT-PL-PEG-FITC. Fluorescence images clearly show SWNT-PL-PEG-FITC translocation into cells (Fig. 2A) even with the complete blockage of the endocytosis pathway. The same results were obtained when these pretreated cells were incubated with SWNT-PL-PEG-FITC of different concentrations (Fig. S3, Supporting Information). It is apparent that endocytosis is not involved during translocation of SWNTs into mitochondria, since their internalization is not affected by the complete blockage of endocytosis either by low temperature or by NaN_3. These results support the reported pathway of SWNTs via passive diffusion across cell membranes[6,18].

We also investigated the impact of mitochondrial transmembrane potential ($\Delta\Psi m$) on the mitochondrial accumulation of transmembranal SWNTs. HeLa cells stained with tetramethylrhodamine methyl ester (TMRM), a $\Delta\Psi m$ indicator, were incubated with SWNT-PL-PEG-FITC for 30 minutes, followed by treatment with staurosporine (STS), a chemotherapeutic agent, to interrupt $\Delta\Psi m$. The $\Delta\Psi m$ started a gradual decrease about 3 hours after STS treatment and led to cell death after its total collapse, as shown in Fig. S4 (Supporting Information). Before STS treatment, the fluorescence emission of FITC showed that SWNT-PL-PEG were entirely distributed in the mitochondria (top panel, Fig. 2B). Three hours after STS treatment, SWNT-PL-PEG-FITC started to separate from mitochondria, accompanied with the decrease of $\Delta\Psi m$ (middle panel, Fig. 2B). Six hours after STS treatment, $\Delta\Psi m$ completely collapsed and SWNT-PL-PEG-FITC diffused into the entire cell (bottom panel, Fig. 2B). These results indicate that the mitochondrial localization of SWNT-PL-PEG-FITC is $\Delta\Psi m$ -dependent.

We used folate (FA) and $\alpha_v\beta_3$ to determine whether SWNTs could be selectively internalized into cancer cells with specific tumor markers, such as folate receptor (FR) and integrin on the tumor cell surface. We found that SWNT-PL-PEG-FA could enter into the FR positive cells (FR+ HeLa cells), but not the FR negative cells (FR- HeLa cells). We also found that SWNT-PL-PEG-$\alpha_v\beta_3$ could enter into the integrin positive cells (U87-MG cells), but not the integrin negative cells (MCF7 cells). The fluorescence emissions of SWNT-PL-PEG-FA or SWNT-PL-PEG-$\alpha_v\beta_3$ from the cells coincided with that of CFP-lamp, indicating that SWNTs are localized in lysosomes (Fig. S5, Supporting Information).

Fluorescence emissions of bovine serum albumin (BSA), a large non cell-targeting molecule, as well as the fluorescence emissions of SWNT-PL-PEG-BSA from the cells, coincided with that of CFP-lamp (Fig. 3A), indicating that both BSA and SWNT-PL-PEG-BSA are localized in lysosomes due to the endocytosis of BSA. In comparison, fluorescence emissions of PI, a small non cell-targeting molecule, were absent from the cells (Fig. 3B, top panel). However, the fluorescence emissions of SWNT-PL-PEG-PI coincide with that of MitoTracker (Fig. 3B, bottom panel), indicating that SWNT-PL-PEG-PI is localized in mitochondria. It is believed that the difference in subcellular localization of PI and SWNT-PL-PEG-PI is due to the electrical properties of SWNTs.

To investigate the possible pathway for the translocation and localization of SWNTs conjugated with different molecules, the same endocytosis-blocking assay was performed. When the cells lost their endocytosis function, cell-targeting molecules ($\alpha_v\beta_3$ and FA) and large molecules (BSA) with their SWNT-PL-PEG conjugates were absent from the cells (Fig. 3C). However, the translocation and localization of small, non cell-targeting molecules (PI) with their SWNT-PL-PEG conjugates were not affected by the blocking of cell endocytosis function.

To explore potential applications of mitochondrial SWNTs, we investigated the direct impact of SWNTs on mitochondria under laser irradiation. HeLa cells were incubated with SWNT-PL-PEG for 2 hours, stained with dicholorofluorescin diacetate (DCFDA) or TMRM, and followed by irradiation with a 980-nm laser. Fluorescence emissions of DCFDA, an indicator of generation of reactive oxygen species (ROS), started in mitochondria (Fig. 4A) and then gradually intensified in the other areas of the cell (Fig. 4B,S6.A-B). Furthermore, in TMRM-stained cells, fluorescence emissions of TMRM decreased after laser irradiation (Fig. 4B,S6.C-D). Fig. 4C shows that laser irradiation of mitochondrial SWNTs could induce cell apoptosis.

The potential biomedical applications of nanotubes require a better understanding of their cellular dynamics. Translocation and localization of SWNTs in cells are among the most important SWNT-cell interactions. Pioneer work by Pantarotto *et al* demonstrated that SWNTs could enter the cytoplasm of normal cells by directly crossing the membrane, using fluorescence microscopy[6]. Seminal work by Porter *et al* recently revealed that SWNTs mainly accumulated in lysosomes of macrophages, using transmission electron microscopy[18]. However, because of phagocytosis, the lysosomal localization of SWNTs in macrophages may not represent typical interactions between SWNTs and other cells, normal or cancerous. Furthermore, TEM imaging of SWNTs is performed under abnormal physiological conditions; SWNTs in living cells may experience different dynamics.

In the current study, we used confocal fluorescence microscopy to observe the dynamics of SWNTs in normal and cancerous cells, as well as in macrophages, under normal physiological conditions. We also conducted mechanistic studies for the subcellular localization of SWNTs in cells. Through fluorescent labeling of all major subcellular components, we pinpointed the mitochondrial localization of SWNT-PL-PEG in living normal and cancerous cells (Fig. 1A and 1B). We also observed the mainly lysosomal

distribution and the minimal mitochondrial localization of SWNT-PL-PEG in macrophages (Fig. 1C).

The mitochondrial localization of SWNT-PL-PEG in cells was disrupted neither by low temperature (4°C) nor by incubation with NaN_3, both being able to inhibit endocytosis (Fig. 2A). These results strongly indicate the transmembranal pathway for mitochondrial localization of SWNT-PL-PEG. We also observed the dispersion of mitochondrial SWNT-PL-PEG into other subcellular components when $\Delta\Psi m$ decreased by the treatment of STS (Fig. 2B). It is known that the mobility of nanotubes can be enhanced by the presence of an electrical potential. For example, nanotube migration in gel electrophoresis medium upon application of a DC electric field has been extensively reported[19]. Specifically, when the nanotubes are charged by association of covalent or non-covalent functionalities, the mobility is greatly enhanced[20]. Based on the observed relationship between $\Delta\Psi m$ and mitochondrial SWNTs in this study, we conclude that SWNT-PL-PEG accumulate in the mitochondria due to the existence of electric potential ($\Delta\Psi m$).

Subcellular localization of surface-modified SWNTs depends on how SWNTs enter the cells. When the conjugated molecules, such as $\alpha_v\beta_3$ and FA, can specifically target tumor cells, they are bound to the cell surface. Their only pathway into the cell is through endocytosis, resulting in the lysosomal distribution of conjugated SWNT-PL-PEG (Fig. S5.A-B). For non cell-targeting molecules, the entry mode depends on the properties of the conjugated molecules. Large molecules, such as BSA, can enter cells only through endocytosis, as shown in Fig. 3A. It is interesting to notice that SWNT-PL-PEG can carry small molecules (such as PI), which cannot enter cells by themselves, and transport them to mitochondria (Fig. 3B). These results provide a basis for selective translocation and localization of SWNT-PL-PEG to desired subcellular components. Such selectivity can facilitate biomedical applications of SWNTs such as drug delivery and phototherapy.

Photothermal therapies for cancer have been widely investigated as a minimally invasive treatment modality in comparison with other methods.[15,21] However, the chromophores in healthy tissue in the light path can also absorb energy, thus reducing the effectiveness of the heat deposition within tumor cells and increasing nonspecific injury of adjacent healthy tissue. *In situ* light-absorbing probes have been used to selectively increase the thermal destructions in the target tumors.[22,23] One application of the mitochondrial SWNTs is selective photothermal therapy. Fig. 4 shows the effectiveness of mitochondrial SWNTs in inducing cell apoptosis under laser irradiation. Such effect is similar to that of photodynamic therapy using mitochondrial photosensitizers such as photofrin[24,25], which is an important adjuvant therapy for cancer. It has also been reported that SWNTs have a differential uptake by tumors[8]. More importantly, use of mitochondrial SWNTs for cancer treatment could avoid phototoxicity. Therefore, laser-SWNTs could become an effective treatment modality for cancer, as a mitochondrial targeting photo-thermal conversion probe.

In conclusion, we have demonstrated for the first time that SWNT-PL-PEG were able to localize in mitochondria of normal and cancerous cells, and that mitochondrial SWNTs are linked to mitochondrial transmembrane potential. We also demonstrated that SWNT-PL-PEG could be localized in different subcellular components by conjugations of different

molecules. The determination and manipulation of subcellular translocation and localization of SWNTs could benefit the design and development of SWNT-assisted therapies.

Supplementary Material

Refer to Web version on PubMed Central for supplementary material.

Acknowledgments

This research is supported by the National Basic Research Program of China (2010CB732602), the Program for Changjiang Scholars and Innovative Research Team in University (IRT0829), the Key Program of NSFC-Guangdong Joint Funds of China (U0931005), and the National Natural Science Foundation of China (30870676; 30800261), and by the US National Institutes of Health (P20 RR016478 from the INBRE Program of the National Center for Research Resources). The authors thank Professor Daniel E. Resasco of the University of Oklahoma for providing CoMoCAT SWNT and performing the AFM/TEM experiments.

References

1. Liu Z, Tabakman SM, Welsher K, Dai H. Nano Research. 2009; 2:85–175. [PubMed: 20174481]
2. Kostarelos K, Bianco A, Prato M. Nature Nanotech. 2009; 4(10):627–633.
3. Chen RJ, Bangsaruntip S, Drouvalakis KA, Kam NWS, Shim M, Li Y, Kim W, Utz PJ, Dai H. Proc Natl Acad Sci USA. 2003; 100(9):4984–4989. [PubMed: 12697899]
4. Gooding JJ, Wibowo R, Liu J, Yang W, Losic D, Orbons S, Mearns FJ, Shapter JG, Hibbert DB. J Am Chem Soc. 2003; 125(30):9006–9007. [PubMed: 15369344]
5. Baughman RH, Zakhidov AA. Science. 1999; 284(5418):1340–1344. [PubMed: 10334985]
6. Pantarotto D, Briand JP, Prato M, Bianco A. Chem Commun. 2004; 7(1):16–17.
7. Kam NWS, Jessop TC, Wender PA, Dai H. J Am Chem Soc. 2004; 126(22):8650–8651. [PubMed: 15250707]
8. Liu Z, Chen K, Davis C, Sherlock S, Cao Q, Chen X, Dai H. Cancer Res. 2008; 68(16):6652–6660. [PubMed: 18701489]
9. Feazell RP, Nakayama-Ratchford N, Dai H, Lippard SJ. J Am Chem Soc. 2007; 129(27):8438–8439. [PubMed: 17569542]
10. Bianco A, Kostarelos K, Prato M. Curr Opin Chem Bio. 2005; 9(6):674–679. [PubMed: 16233988]
11. Liu Y, Wu DC, Zhang WD, Jiang X, He CB, Chung TS, Goh SH, Leong KW. Angew Chem Int Ed. 2005; 44(30):4782.
12. Kam NWS, Liu Z, Dai HJ. Am Chem Soc. 2005; 127(36):12492–12493.
13. Kam NWS, Liu Z, Dai H. Angew Chem Int Ed. 2006; 45(4):577–581.
14. Kam NWS, O'Connell M, Wisdom JA, Dai H. Proc Natl Acad Sci USA. 2005; 102(33):11600–11605. [PubMed: 16087878]
15. Zhou FF, Xing D, Ou ZM, Wu BY, Resasco DE, Chen WRJ. Biomed Opt. 2009; 14(2):021009.
16. Zhang M, Ajima K, Tsuchida K, Sandanayaka ASD, Ito O, Iijima S, Yudasaka M. Proc Natl Acad Sci USA. 2008; 105(39):14773–14778. [PubMed: 18815374]
17. Welsher K, Liu Z, Daranciang D, Dai H. Selective probing and imaging of cells with single walled carbon nanotubes as near-infrared fluorescent molecules. Nano Lett. 2008; 8(2):586–590. [PubMed: 18197719]
18. Porter AE, Gass M, Muller K, Skepper JN, Midgley PA, Welland M. Nature nanotech. 2007; 2(11):713–717.
19. Vetcher AA, Srinivasan S, Vetcher IA, Abramov SM, Kozlov M, Baughman RH, Levene SD. Nanotech. 2006; 17(16):4263–4269.
20. Usrey ML, Nair N, Agnew DE, Pina CF, Strano MS. Langmuir. 2007; 23(22):7768. [PubMed: 17530869]
21. Amin Z, Donald JJ, Masters A, Kant R, Steger AC, Bown SG, Lees WR. Radiology. 1993; 187:339–347. [PubMed: 8475270]

22. Chen WR, Adams RL, Bartels KE, Nordquist RE. Cancer Lett. 1995; 94:125–131. [PubMed: 7634239]
23. Loo C, Lowery A, Halas N, West J, Drezek R. Nano Lett. 2005; 5:709–711. [PubMed: 15826113]
24. Wu Y, Xing D, Luo S, Tang Y, Chen Q. Cancer Lett. 2006; 235(2):239–247. [PubMed: 15958279]
25. Wu Y, Xing D, Chen WR. Cell Cycle. 2006; 5(7):729–734. [PubMed: 16627992]

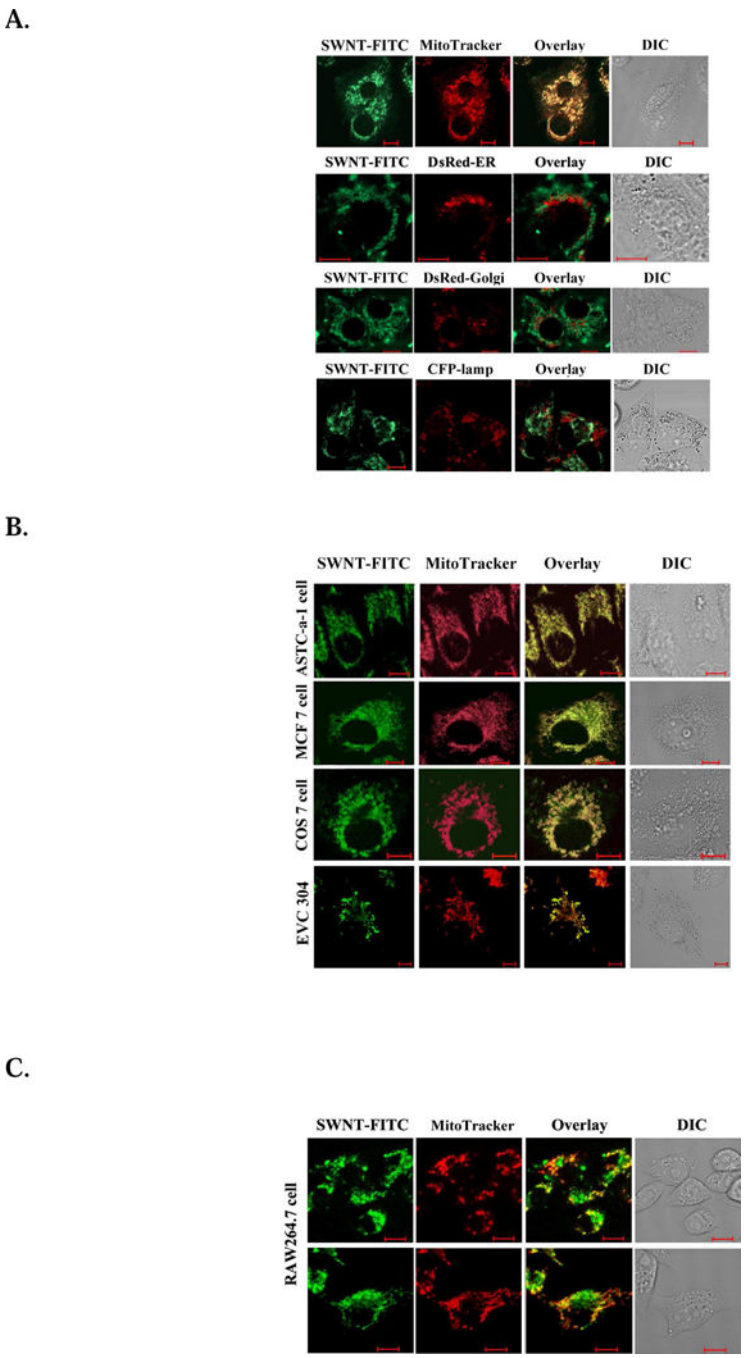

Figure 1.

Localization of SWNT-PL-PEG in subcellular components of different cells. **A**. Localization of SWNT-PL-PEG in different subcellular components of HeLa cells. Cells (5×10^4 per well) transfected with DsRed-ER, DsRed-Golgi, CFP-lamp, or stained with MitoTracker were incubated with SWNT-PL-PEG-FITC (2.5 μg/ml) for 30 minutes. Confocal images of the cells show that SWNT-PL-PEG-FITC is localized in the mitochondria, but not in ER, Golgi, or lysosomes. **B**. Mitochondrial localization of SWNT-PL-PEG in different cells. Cells (ASTC-a-1, MCF 7, COS 7, EVC304) were stained by MitoTracker and incubated with

SWNT-PL-PEG-FITC for 30 minutes. Confocal images of the cells show consistent mitochondrial localization of SWNT-PL-PEG-FITC in all cells. **C**. Lysosomal localization of SWNT-PL-PEG in macrophages. Cells transfected with CFP-lamp and stained with MitoTracker were incubated with SWNTs-PL-PEG-FITC for 30 minutes. Confocal images of the cells show that SWNT-PL-PEG-FITC is mainly localized in the lysosome.

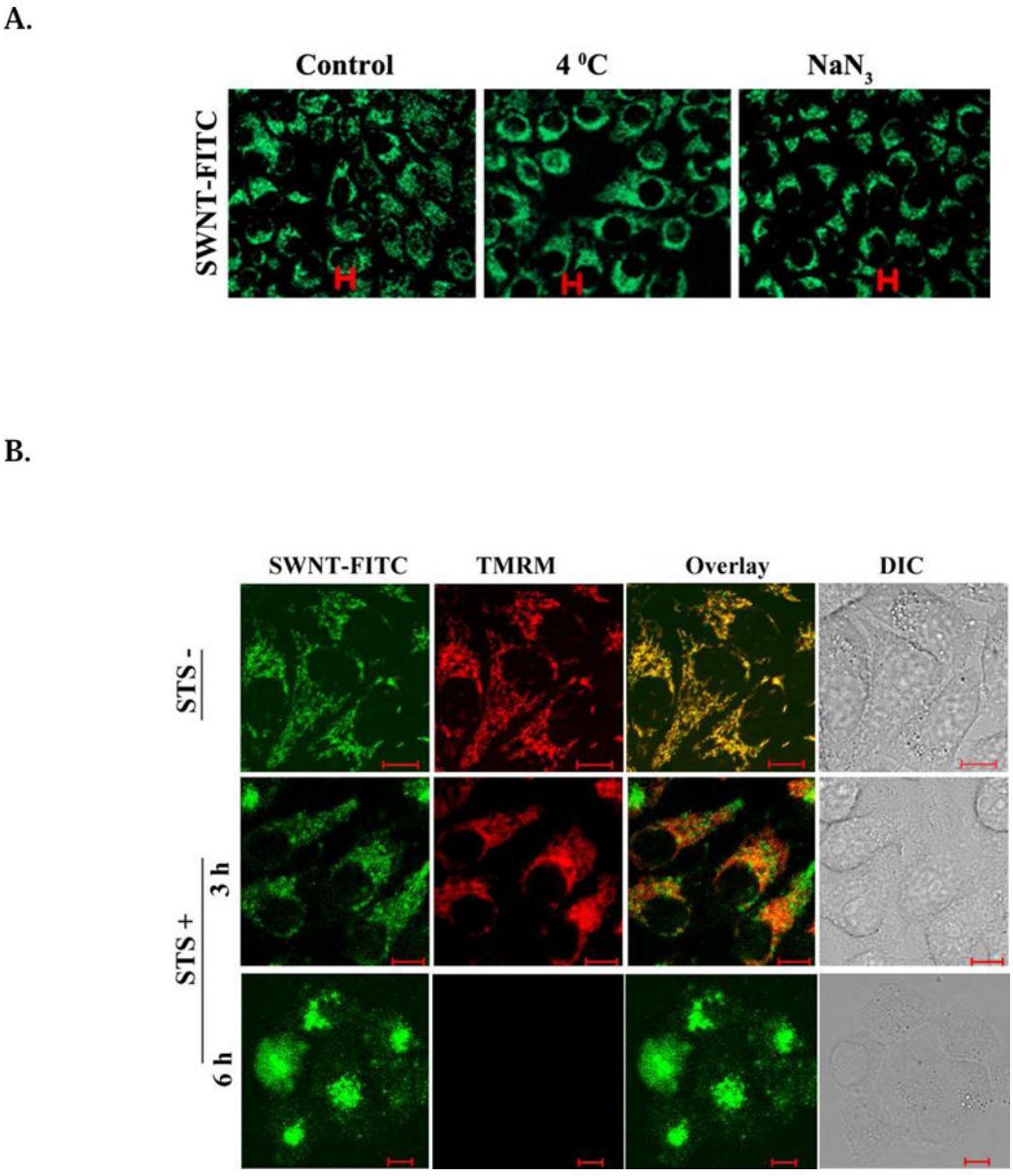

Figure 2.

Mitochondrial localization of SWNT-PL-PEG after blocking the cell phagocytosis pathway. **A**. Distribution of mitochondrial SWNT-PL-PEG in HeLa cells incubated at 4°C or with NaN_3. Fluorescent images of cells after incubation with SWNT-PL-PEG-FITC (2.5 μg/ml) at 4°C or after pretreatment with NaN_3 show SWNT-PL-PEG-FITC translocation into the cells, excluding the endocytosis pathway. **B**. Effect of ΔΨm on the subcellular localization of SWNT-PL-PEG. TMRM-stained HeLa cells were incubated with SWNT-PL-PEG-FITC (2.5 μg/ml) for 30 minutes, followed by the treatment of STS. Confocal images of the cells after the treatment show that as ΔΨm decreases the mitochondrial SWNTs disperse gradually into cytoplasma.

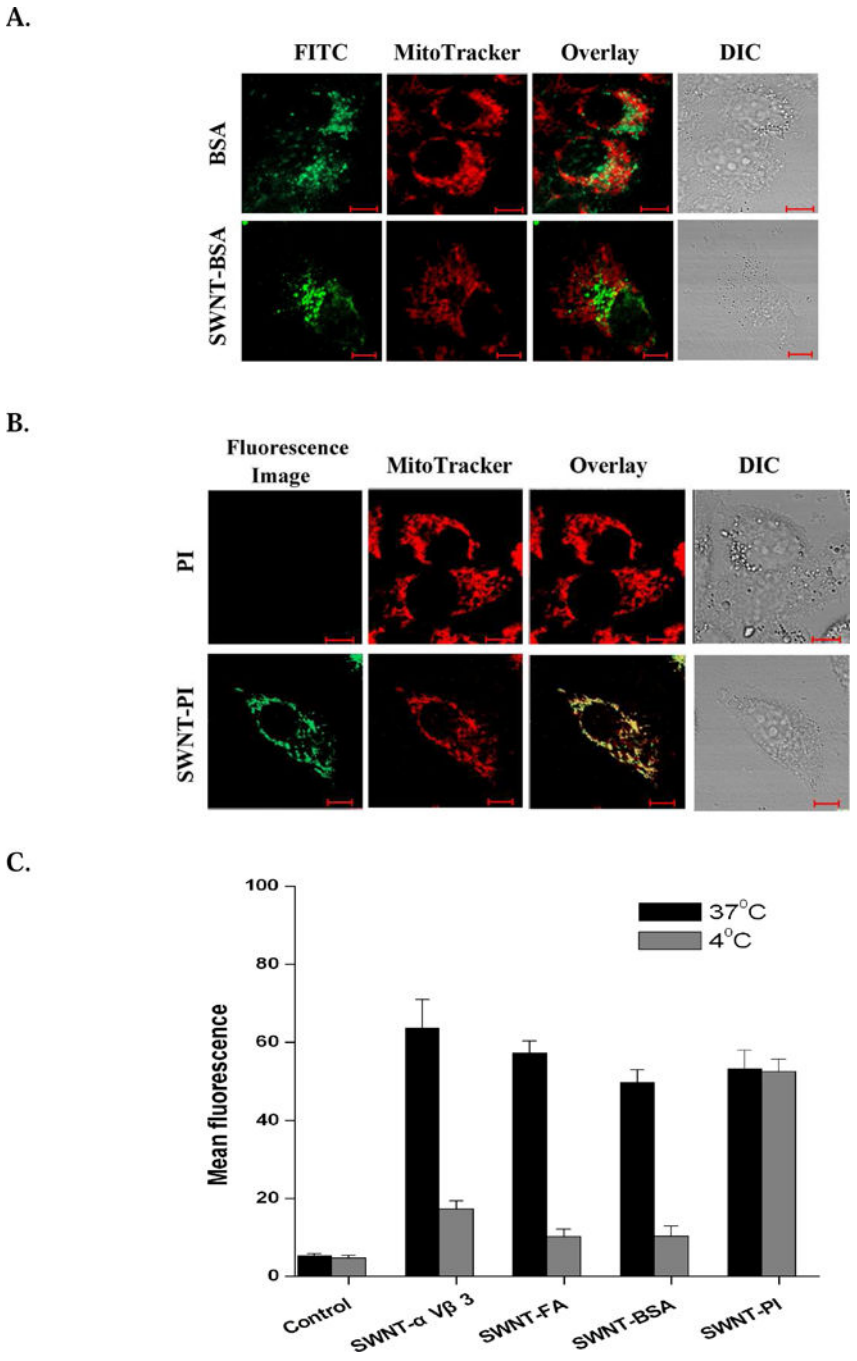

Figure 3.

Subcellular localization of surface-modified SWNTs. **A**. Subcellular localization of BSA-FITC and SWNT-PL-PEG-BSA-FITC in HeLa cells. Cells transfected with CFP-lamp and stained with MitoTracker were incubated with BSA-FITC (1 μg/ml of BSA) or SWNT-PL-PEG-BSA-FITC (2.5 μg/ml of SWNTs) for 30 minutes. Confocal images of the cells show that BSA-FITC and SWNT-PL-PEG-BSA-FITC are mainly localized in the lysosome. **B**. Subcellular localization of PI and SWNT-PL-PEG-PI in HeLa cells. Cells transfected with CFP-lamp and stained with MitoTracker were incubated with PI (5 μg/ml) or SWNT-PL-

PEG-PI (2.5 μg/ml of SWNTs) for 30 minutes. Confocal images of the cells show that SWNT-PL-PEG-PI is mainly localized in the mitochondria. **C**. Statistical analysis of fluorescence emission intensity of surface-modified SWNTs in cells incubated at 37°C or 4°C. Only small, non surface-targeting molecules (PI) can be carried by SWNTs into the mitochondria without being affected by the loss of cell endocytosis function. Bars, means SD (n=5).

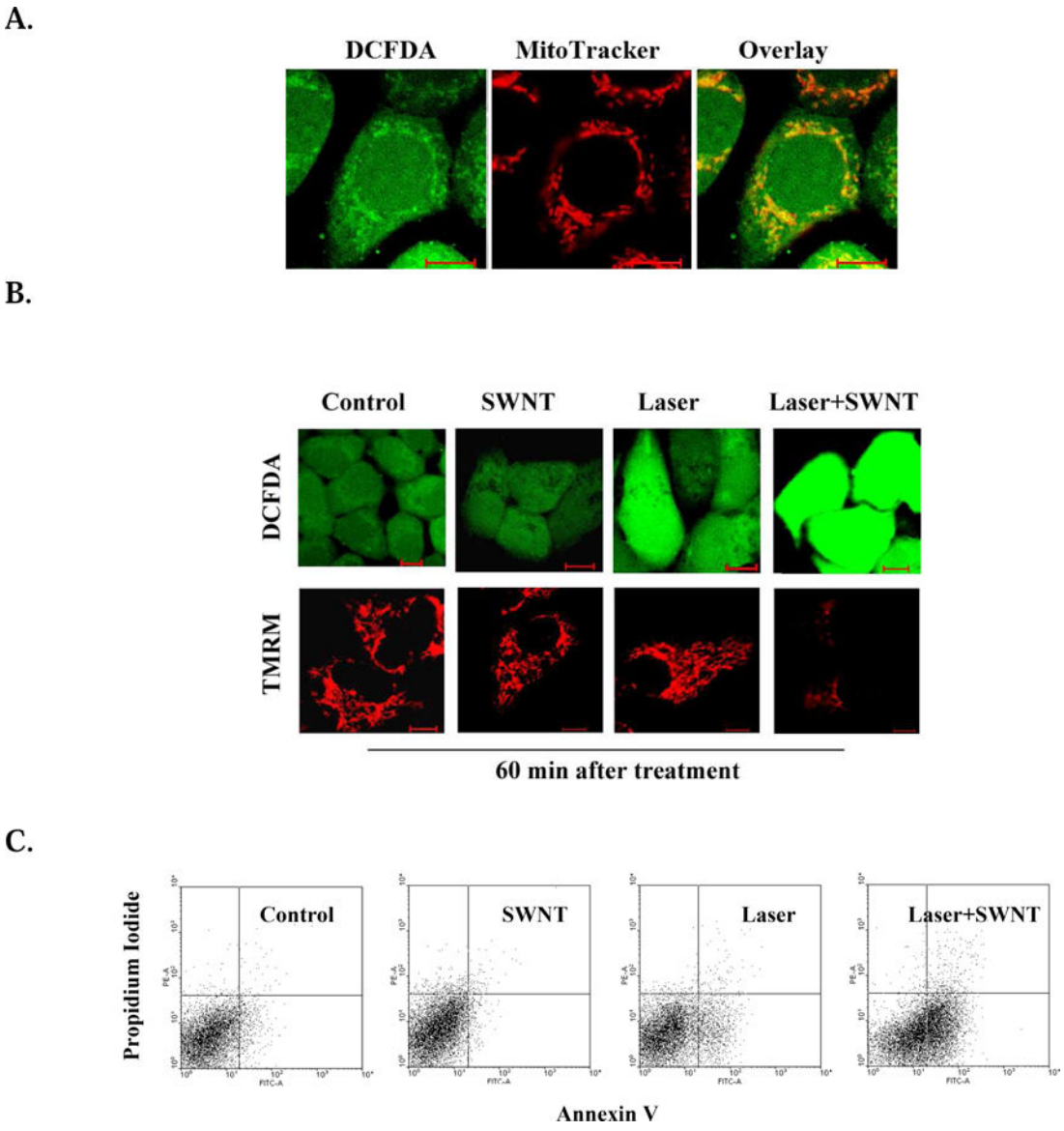

Figure 4.

Apoptosis induced by mitochondrial SWNTs under laser irradiation. HeLa cells were incubated with SWNT (2.5 μg/ml) for 2 hours, then irradiated with a 980 nm laser (0.75 W/cm^2) for 2 minutes. **A**. Initial ROS generation in the mitochondria after laser irradiation. **B**. ROS generation and ΔΨm changes in the cells at different time points after treatment. Fluorescent image series of H_2DCFDA and TMRM were acquired after different treatments. **C**. Cell apoptosis induced by different treatments. Cells harvested 6 hours after different treatments were double stained by Annexin V and PI, and analyzed by FACS.